Previously hidden low-energy ions: a better map of near-Earth space and the terrestrial mass balance



2015 Phys. Scr. 90 128005

(http://iopscience.iop.org/1402-4896/90/12/128005)

OPEN ACCESS
IOP Publishing | Royal Swedish Academy of Sciences Physica Scripta
Phys. Scr. **90** (2015) 128005 (11pp) doi:10.1088/0031-8949/90/12/128005

## Invited Comment

# Previously hidden low-energy ions: a better map of near-Earth space and the terrestrial mass balance

**Mats André**

Swedish Institute of Space Physics, Uppsala, Sweden

E-mail: mats.andre@irfu.se

Received 13 May 2015, revised 7 September 2015
Accepted for publication 7 October 2015
Published 19 November 2015

**Abstract**

This is a review of the mass balance of planet Earth, intended also for scientists not usually working with space physics or geophysics. The discussion includes both outflow of ions and neutrals from the ionosphere and upper atmosphere, and the inflow of meteoroids and larger objects. The focus is on ions with energies less than tens of eV originating from the ionosphere. Positive low-energy ions are complicated to detect onboard sunlit spacecraft at higher altitudes, which often become positively charged to several tens of volts. We have invented a technique to observe low-energy ions based on the detection of the wake behind a charged spacecraft in a supersonic ion flow. We find that low-energy ions usually dominate the ion density and the outward flux in large volumes in the magnetosphere. The global outflow is of the order of $10^{26}$ ions $s^{-1}$. This is a significant fraction of the total number outflow of particles from Earth, and changes plasma processes in near-Earth space. We compare order of magnitude estimates of the mass outflow and inflow for planet Earth and find that they are similar, at around 1 kg $s^{-1}$ (30 000 ton $yr^{-1}$). We briefly discuss atmospheric and ionospheric outflow from other planets and the connection to evolution of extraterrestrial life.

Keywords: low-energy ions, atmospheric outflow, terrestrial mass balance

(Some figures may appear in colour only in the online journal)

## 1. Introduction

Space is not empty. The sun is emitting not only electromagnetic radiation but also a solar wind. This unsteady wind includes charged particles (a plasma) and a magnetic field. When this supersonic wind hits the magnetic field of the Earth and is deflected, an enormous cavity is created, the magnetosphere. The visible aurora was studied for hundreds of years without realizing that this phenomenon is caused by charged particles accelerated at several thousand kilometers altitude within the magnetosphere, which then hit the atmosphere (Gilmore 1997, Brekke and Broms 2013). Studies of plasma in the solar wind and the magnetosphere are today closely linked to investigations of laboratory, fusion and astrophysical plasmas (Kivelson and Russell 1995, Aschwanden 2004, Koepke 2008, Koskinen 2011).

A consequence of solar radiation and the solar wind is that matter can escape from planet Earth. In the following we consider ions leaving Earth and discuss how these particles change the properties of near-Earth space. We then compare this outflow with the outflow of neutrals and with the inflow of meteoroids and larger objects.

More than a hundred years ago, magnetic field observations on the ground, and reflections of radio waves, showed the existence of currents and charged particles in what would

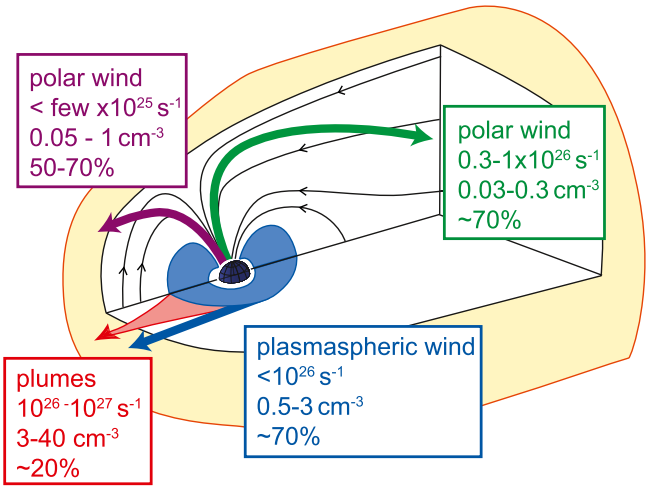


**Figure 1.** Sketch of the magnetosphere. Including low-energy ions gives a better map of near-Earth space. The solar wind (from left) creates a bow shock (not shown) and a magnetopause. Regions where the density is dominated by low-energy ions are indicated. Sources are indicated, together with order of magnitude outflow rates and densities, and percentage of the time that low-energy ions dominate outside the ionosphere and plasmasphere. The polar wind mostly flows into the tail with a typical outflow rate of about $10^{26}$ ions $s^{-1}$. Some tens of percent of this flow can be diverted through the dayside magnetopause. The plasmaspheric wind contributes an outflow comparable to the polar wind, but only through a limited area of the magnetopause. Dayside plumes occur much less frequently, but transfer a large mass of ions when they do occur (André and Cully 2012).

become known as the ionosphere. Before the launch of the first satellites, studies of natural electromagnetic so-called whistler waves indicated the presence of the plasmasphere (Gillmore 1997), figure 1. The ionospheric plasma is created by ionization of the upper atmosphere at altitudes of about eighty to several hundred km by solar UV and EUV radiation, and to some extent by precipitating particles, including auroral electrons at energies from one to tens of keV. The peak plasma density is about $10^6$ $cm^{-3}$ near noontime in the so-called F-layer at about 250 km altitude. The thermal plasma energy is of the order of 0.1 eV (about 1000 K), mainly determined by collisions with the denser neutral gas (Kelley 2009). In this simple ionospheric scenario, essentially all ions have velocities well below escape velocity. In comparison with the solar wind, particle energies in the ionosphere are low. The solar wind velocity of at least a few hundred km $s^{-1}$ corresponds to energies of about a keV for the major ion species, $H^+$. In the following we discuss low-energy ions leaving the ionosphere, some being energized to several keV, but a major fraction staying cold also far away from Earth.

While collisions are important in the dense ionosphere at altitudes below about 500 km most of the magnetosphere has much lower density and is essentially collisionless. The charged particles are still strongly coupled via electromagnetic fields. Upstream from Earth a collionless shock is formed at about 90 000 km altitude (15 $R_E$, Earth radii) when the supersonic solar wind is deflected by the terrestrial magnetic field. At around 10 $R_E$ a current sheet, the magnetopause, is separating the shocked solar wind from the regions dominated by the terrestrial magnetic field. Some of the solar wind energy and particles can enter the magnetosphere behind the magnetopause. One major process permitting mass and energy exchange across this plasma boundary is so-called magnetic reconnection (Priest and Forbes 2000, Paschmann *et al* 2013). Plasma can be further energized in the reconnection processes, transferring energy from the magnetic field to particle kinetic energy.

For many years the solar wind was believed to be the obvious source of magnetospheric plasma, which was consistent with observations. In contrast, we have found that the magnetosphere often is dominated by low-energy (eV) plasma of ionospheric origin (figure 1). These ions are hard to detect onboard a sunlit spacecraft in a low-density plasma. The spacecraft emits photoelectrons and in steady state often charges to several tens of volts positive, preventing positive low-energy ions from reaching the onboard detectors. We show how this problem can be solved. Rather than using a particle detector onboard a spacecraft, we observe the electric field caused by a wake behind a spacecraft in a supersonic ion flow. We discuss the contribution of these ions to the overall mass balance of planet Earth. We conclude by considering atmospheric and ionospheric outflow from other planets and the importance for extraterrestrial life.

## 2. Ions in near-Earth space

In the beginning of the space age, scientific spacecraft included instruments to detect high-energy (MeV) particles, leading to the discovery of the so-called Van Allen belts (Van Allen and Frank 1959, Foerstner 2007). These particles are of practical importance since they may damage spacecraft but they contribute only a minor fraction of the mass in the magnetosphere. Later spacecraft detectors could cover the energy range from several eV to hundreds of keV. For a long time it was believed that the magnetosphere was dominated by plasma of solar wind origin. Observations of $O^+$ ions at kev energies (occurring only at very low densities in the solar wind) made it clear that ions flowing out from the ionosphere can contribute to the near Earth plasma (Shelley *et al* 1972, Sharp *et al* 1977). Today the outflow of $H^+$, $O^+$, $He^+$ and other ions from the ionosphere is discussed in review articles and textbooks (André and Yau 1997, Yau and André 1997, Moore and Horwitz 2007). However, these ions typically have energies of at least several eV, while ions at lower energies often have not been possible to detect.

Ions originating in the polar cap ionosphere (regions around the magnetic poles) often have low (eV) energies and can form a supersonic 'polar wind' along 'open' magnetic field lines (connected to the solar wind) expanding into the anti-sunward 'magnetotail' of the magnetosphere (Yau *et al* 2007). Such a supersonic outflow of low-energy ions was predicted by Axford (1968) and Banks and Holzer (1968). Early observations of this outflow were made at altitudes up to a few thousand kilometers by the Explorer 31 (Hoffman 1970) and DE-1 satellites (Chandler *et al* 1991).

Many of the following studies of the high-latitude ion outflow, including the polar wind, used observations up to several $R_E$ by the Akebono, DE-1 and Polar spacecraft (Yau and André 1997, Cully *et al* 2003, Abe *et al* 2004, Huddleston *et al* 2005, Peterson *et al* 2006, Yau *et al* 2007). The source of the polar wind can also be observed from the ground by radars, up to altitudes of several hundred kilometers (Ogawa *et al* 2009). $H^+$, $O^+$ and other ions originating in the auroral region equatorward of the polar cap can typically reach higher (keV) energies due to various energization processes (André and Yau 1997, Moore and Horwitz 2007). Due to convection, keV ions from the dayside can appear also above the polar cap. Observations of such ions by the Cluster spacecraft cover altitudes up to about 20 $R_E$ (Nilsson *et al* 2012, Nilsson *et al* 2013, Liao *et al* 2012). However, concerning low-energy ions, at altitudes above a few $R_E$ observations of such ions onboard a sunlit and charged spacecraft, have been rare.

Ions originating from the equatorial ionosphere often end up in the plasmasphere. This is a torus-like region with low-energy (eV) and dense (compared to the rest of the magnetosphere) plasma of ionospheric origin, on nearly dipolar magnetic field lines. In the plasmasphere, plasma co-rotates with the Earth, while plasma outside its outer boundary (the plasmapause) is controlled by magnetospheric convection. The plasmapause is typically located inside geostationary orbit at 6.6 $R_E$ for moderate magnetic activity (Borovsky and Denton 2008, Darrouzet *et al* 2008, 2009). At high geomagnetic activity the outer regions of the plasmasphere (around 50% of the mass) are removed by increased magnetospheric convection, forming plumes. Plumes are usually found in the afternoon and last for days, but weaken in density, width and flux with time (Chandler *et al* 1999, Borovsky and Denton 2008, Darrouzet *et al* 2008, 2009, Moore *et al* 2008, Spasojevic and Sandel 2010). Low-energy ions are found just inside the magnetopause, not only in plasmaspheric plumes (Matsui *et al* 1999, André and Lemaire 2006, Lee and Angelopoulos 2014), and indications of a cold 'plasmaspheric wind' have been found (Dandouras 2013). However, as for the high latitude case, observations of low-energy ions onboard a sunlit, and charged spacecraft have been rare.

## 3. The problem of hidden low-energy ions

In our definition, low-energy ions have thermal energies, and drift energies relative to Earth, of less than tens of eV. These ions are hard to detect onboard a sunlit spacecraft in a low-density plasma. The spacecraft emits photoelectrons and in steady state often charges to several tens of volts positive, preventing positive low-energy ions from reaching the onboard detectors. There have still been suggestions for a few decades that low-energy ions of ionospheric origin can be a significant source of magnetospheric plasma (Chappell *et al* 1980, 1987, Olsen 1982, Olsen *et al* 1985, Chappell 2015). However, in most of the magnetosphere it has not been possible to get more than glimpses of this low-energy population.

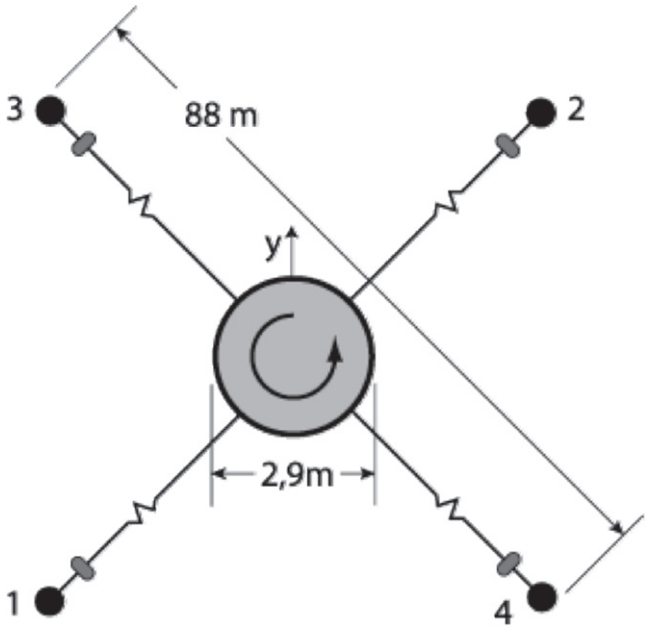


**Figure 2.** The electric field and wave (EFW) instrument has four wire booms mounted on each of the Cluster spacecraft. The distance from the satellite centre to the boom tip is 44 m. The satellite spins at a rate of once every four seconds, which keeps the booms taut. The actual sensor is a sphere, 8 cm in diameter, at the end of each boom.

For comparison, in the ionosphere the density is often high enough that the electrons in the plasma will cause the spacecraft to charge negatively. Here an ion detector can determine thermal energies of a few tenths of an eV and upflow velocities of a few hundred $m\,s^{-1}$ (Burchill *et al* 2010).

## 4. The way to a solution

Combining data analysis and simulations we have invented a new method to detect low-energy (eV) positive ions from the ionosphere on a positively charged (tens of volts) spacecraft. One important part of the new method is the electric field and wave (EFW) instruments on the four Cluster spacecraft. EFW uses two pairs of spherical probes deployed on wire booms in the satellite spin plane to measure the electric field, figure 2 (Gustafsson *et al* 2001, Eriksson *et al* 2006). The probe-to-probe separation is 88 m. The instrument can be used to obtain the electric field by taking the potential difference between two probes. We also use measurements of the potential difference between the probes and spacecraft, often refereed to as the spacecraft potential, to estimate the plasma density (Pedersen *et al* 2008, Lybekk *et al* 2012).

The Cluster spacecraft were launched in two pairs during the summer of 2000 (Escoubet *et al* 2001). After launch the EFW instruments performed well and mainly as expected. However, in large regions in the magnetotail lobes (regions with low density plasma magnetically connected to the polar caps) the observations did not make sense. We expected the lobes to be regions of low activity and with small electric

fields. However, rather often large regions with electric fields of several mV $m^{-1}$ were observed. Although this may at first seem to be small fields, particles accelerated in such an electric field over thousands of kilometers (smaller than the typical lengths scales in this region) would gain keV energies. These particles would easily be detected by onboard particle detectors. One hint to what was going on was that no such high energy particles were observed. Another hint was that when the spacecraft potential control instrument ASPOC was on, the EFW fields looked reasonable. ASPOC emits an ion beam to reduce spacecraft charging, which is beneficial for direct particle observations (Torkar *et al* 2001). In addition, when ASPOC was on, our observations agreed well with the electron drift instrument (EDI) electric field instrument (Paschmann *et al* 2001). This instrument is detecting the quasi-static electric field based on a completely different technique: the field is inferred by measuring the drift of artificially emitted high-energy (keV) electrons as they gyrate back to the spacecraft under the influence of the geophysical magnetic field. In the lobes, these electrons have gyroradii of several kilometers, much longer than the EFW wire booms (Eriksson *et al* 2006). Although it at first seems contradictory, it turns out that both electric field instruments give correct values also when ASPOC is off.

What started out as a dedicated attempt to understand the EFW instrument performance turned out to initiate a new way to detect low-energy ions. The key is that EFW and EDI measure the electric field in different regions. EFW locally (order 100 m) around the spacecraft and EDI averaged over much larger distances (few km). Much of the initial work on this method, and on the geophysical importance of low-energy ions, was performed by Anders Eriksson and his graduate student Erik Engwall (Engwall *et al* 2006a, 2006b, Eriksson *et al* 2006, Engwall *et al* 2009a, 2009b).

## 5. The solution

Plasma flowing past a spacecraft will create a wake downstream of this obstacle, as has been studied from the beginning of the space age (e.g., Kraus and Watson 1958, Rand 1960). However, most earlier wake studies are not directly applicable to the case of a positively charged spacecraft in a low-density supersonic polar wind.

Low-energy positive ions in a supersonic flow can create an enhanced wake behind a positively charged spacecraft. Here the ions are diverted not by the mechanical structure but rather by the surrounding potential structure (Engwall *et al* 2006a, Miyake *et al* 2013). This enhanced wake can be much larger than the direct wake caused by particles hitting the spacecraft. The conditions for the enhanced wake formation sketched in figure 3 (top) are that the ion flow energy $mv^2/2$ not only exceeds the thermal energy $KT$ but also is lower than the equivalent energy of the spacecraft potential $eV_{SC}$

$$KT < mv^2/2 < eV_{SC}. \quad (1)$$

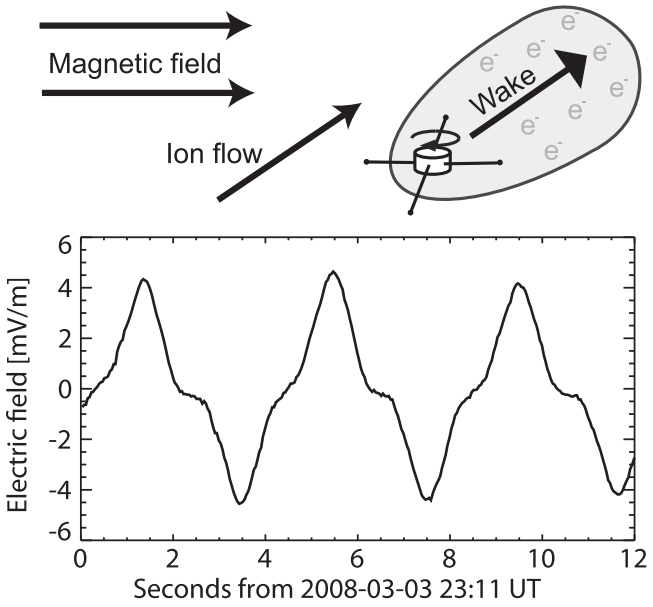


**Figure 3.** (top) Sketch of the wake behind a positively charged Cluster spacecraft, caused by a supersonic flow of cold ions. (bottom) Non-sinusoidal electric field measured by the electric field instrument booms on a Cluster spacecraft, in a supersonic flow of cold ions (André and Cully 2012, André *et al* 2015).

The ion wake will be filled with electrons, whose thermal energy is higher than the ram kinetic energy, in contrast to that of the ions. Due to the large geometric dimensions of the enhanced wake, the negative space charge density can then create a substantial local wake electric field close to the spacecraft. For typical parameters in the polar wind, the local wake has a scale length of 100 m. The wake electric field can be observed with the EFW wire boom instrument, while the electrons emitted by EDI have a much larger gyroradius and are not significantly affected.

For a given velocity, lighter ions such as $H^+$ will be more affected by the spacecraft and hence create a larger wake. Figure 3 (bottom) shows an example of a wake electric field observation. The non-sinusoidal repetitive pattern is due to the wake, and the 4 s spin of the spacecraft, and indicates the presence of low-energy ions (Engwall *et al* 2006a, 2006b, 2009a, 2009b, André *et al* 2010).

The electric field observed by the EFW wire boom instrument is a combination of the geophysical and the wake electric fields. The wake electric field is obtained as the difference between the local electric field at the spacecraft (observed by EFW) and the geophysical quasi-static electric field (EDI). The perpendicular $\mathbf{E} \times \mathbf{B}$ ion drift is given by the geophysical electric field and the ambient magnetic field observed by the fluxgate magnetometer (FGM) (Balogh *et al* 2001). Assuming that the ions are unmagnetized on the wake length scale, the direction of the wake electric field gives the direction of the flow. Since the perpendicular velocity component of the flow is known, the parallel component can be inferred. This technique has been verified in the magnetotail (Engwall *et al* 2006b), studied with simulations

(Engwall *et al* 2006a), and is further discussed by Engwall *et al* (2009b).

The plasma density can be estimated by calibrating observations of the spacecraft potential obtained by the Cluster EFW instrument (Pedersen *et al* 2008, Svenes *et al* 2008, Lybekk *et al* 2012, Haaland *et al* 2012b).

In summary, the presence of a supersonic flow of low-energy ions can be inferred by detecting a wake electric field, obtained as a large enough difference between the quasi-static electric fields observed by the EFW (total electric field) and EDI (geophysical electric field) instruments. To estimate the drift velocity, observations of the perpendicular $\mathbf{E} \times \mathbf{B}$ drift velocity from the geophysical quasi-static electric field (EDI) and the geophysical magnetic field (FGM) are needed, together with the direction of the wake electric field. The ion flux can then be estimated from the drift velocity and the density. Details concerning the data analysis are given by Engwall *et al* (2009b) and André *et al* (2015).

## 6. Low-energy ions and a better map of near-Earth space

The new 'wake' method to detect low-energy ions has been used to map these ions both in the magnetotail lobes (Engwall *et al* 2009a, 2009b, André *et al* 2015) and in the equatorial dayside region (André and Cully 2012). The improved map of near-Earth space is shown in figure 1.

To study the outflow of ions from the polar caps into the magnetotail lobes, André *et al* (2015) used two Cluster spacecraft and ten years of data, 2001–2010, i. e. from the peak of solar cycle 23 to beyond the first minimum of cycle 24. The study includes altitudes from 5 $R_E$ geocentric (about 25 000 km altitude), above the denser plasma where other methods are useful, up to 20 $R_E$, the apogee of the Cluster mission. This is a large data set and even after applying rather strict selection rules on the data to minimize errors, the resulting statistics are good.

To study the occurrence of drifting low-energy ions, a total of 1 680 000 data points (4 s spacecraft spins) can be used to search for a wake. We find wakes indicating low-energy ions in 64% of the data, consistent with earlier studies using smaller data sets (Engwall *et al* 2009a, 2009b). Low-energy ions are common during all parts of the solar cycle (André *et al* 2015).

To quantitatively study the outward flux of low-energy ions, even stricter data selection rules are applied by André *et al* (2015). Using a total of 320 000 data points, they obtain density, outward velocity along the magnetic field, outward ion flux and flux mapped to 1000 km altitude, figure 4. (The flux is mapped downwards to a stronger magnetic field, taking into account the converging magnetic field.) The density increases as a function of increasing solar EUV flux during the solar cycle (as indicated by the F10.7 index, André *et al* 2015) while the parallel velocity does not vary much. The resulting mapped flux increases about a factor of 2 with increased solar EUV.

Our wake method is more sensitive to lighter ion species since for a given velocity their lower energy will make them more affected by the spacecraft potential and thus create a larger wake. Our method can not tell the difference between ion populations with different masses. However, protons are the dominant ion species in the low-energy high-latitude ion outflow (Su *et al* 1998), but the ion composition can vary substantially with geomagnetic and solar activity (e.g. Cully *et al* 2003). As a first approximation, when calculating the ion outflow in the magnetotail, we lower the total density by a factor of 0.8 (Su *et al* 1998, Engwall *et al* 2009b, André *et al* 2015).

To estimate the total outflow, we assume a total polar cap area of 3–6 $\times$ $10^{17}$ $cm^2$ (low to high geomagnetic activity), (Li *et al* 2012, Milan *et al* 2009, 2012). The mapped outward ion flux is about 2 to about 4 $\times$ $10^8$ $cm^{-2}$ $s^{-1}$ (low to high solar EUV, figure 4). This gives a total outflow, from both hemispheres, of about 0.6–2.4 $\times$ $10^{26}$ ions $s^{-1}$, increasing with increasing polar cap size (due to increased geomagnetic activity) and increased solar EUV (André *et al* 2015).

Comparing this low-energy ion outflow observed at high altitude by Cluster with the low-energy ion outflow observed at low altitude (where spacecraft charging is less of a problem) shows good agreement (Peterson *et al* 2008). At high altitudes, the low-energy ion outflow is higher than the hot ion outflow, see tables of Peterson *et al* (2006) and Engwall *et al* (2009a) for a comparison of spacecraft, energies and altitudes.

To detect low-energy ions at the dayside magnetopause, André and Cully (2012) used three complete seasons of Cluster dayside coverage (November 2006 through July 2009). This allows studies of both high-latitude and low-latitude locations on the dayside magnetopause. Two hours of data (about 1 $R_E$ for a stationary magnetopause) just inside a total of 370 magnetopause crossings was searched for low-energy ions. Three methods were used. The first was based on the detection of a spacecraft wake to find low-energy ions. The second method was based on the fact that occasionally strong electric fields occur close to the magnetopause, accelerating cold ion populations into onboard particle detectors. Such observations can be used to put rough lower bounds on the occurrence of low-energy ions. The third method was to compare partial density moments from onboard particle detectors with density estimates from observations of waves at the plasma frequency. (The plasma frequency is a resonant frequency, proportional to the square root of the density.) The findings are summarized in figure 1.

On the dayside, the outflow of low-energy ions is very variable. When plasmaspheric plumes are not present, the outflow is typically a few times $10^{25}$ ions $s^{-1}$ integrated over the dayside. In plumes (occurring about 20% of the time) the outflow can be up to $10^{27}$ ions $s^{-1}$. Our new results show that low-energy ions can dominate 50%–70% of the time just inside the magnetopause, even when there are no plasmaspheric plumes.

The results in figure 1 give an updated map of the magnetosphere, showing that low-energy ions dominate the density and number flux for large volumes in the

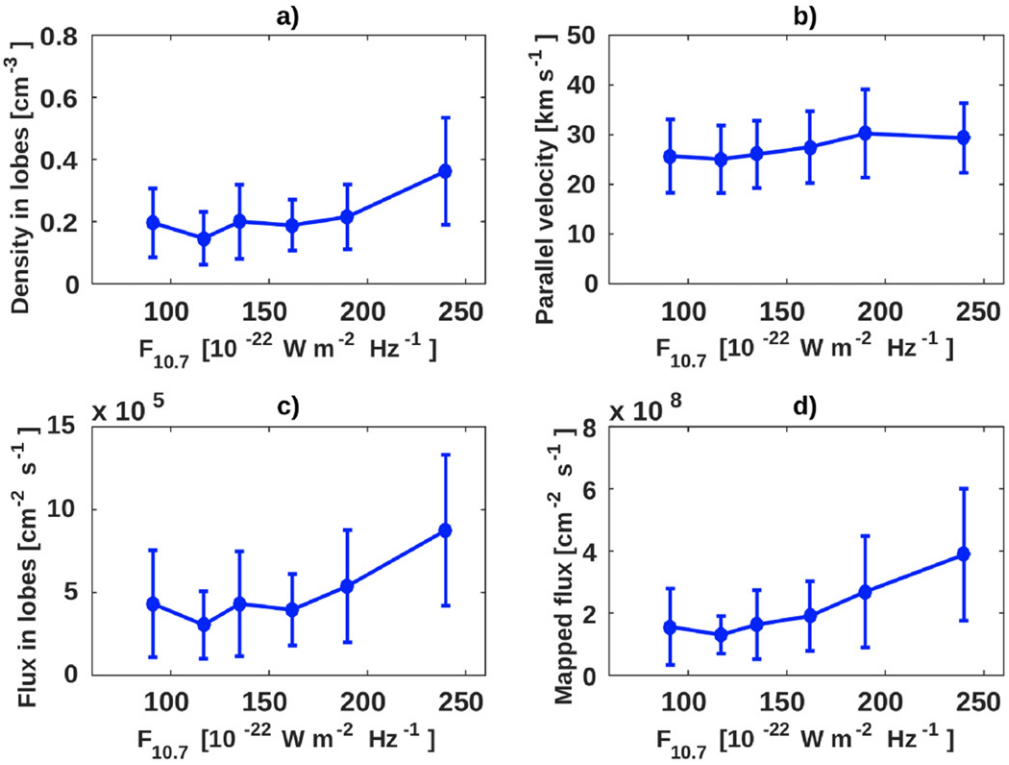


**Figure 4.** (a) low-energy ion density as a function of solar EUV radiation (estimated from the parameter $F_{10.7}$), (b) outward velocity parallel to the magnetic field, (c) outward local flux in the magnetotail lobes, (d) outward flux mapped to an altitude of 1000 km. The bars show the geophysical variations in the data, indicated by ±0.5 standard deviation. The plotted average values each include an equal fraction of the total of 320 000 data points. The density increases by about a factor of 2 with increasing solar EUV, while the velocity does not change much. The resulting flux increases by a factor of 2 (André *et al* 2015).

magnetosphere, a large fraction of the time. The change in density gives a change in the Alfvén velocity (inversely proportional to the square root of the density) and hence in the velocity of much energy transfer in the plasma. This velocity change also affects the rate of energy conversion in magnetic reconnection. Low-energy ions also change how the microphysics of magnetic reconnection works since the gyro-radius introduces a new length-scale between the gyro-radii of electrons and hot ions (André *et al* 2010, Toledo-Redondo *et al* 2015).

## 7. Outflow of ions

The average global outflow of $H^+$ is of the order of $10^{26}$ ions s$^{-1}$. Concerning the outflow of $He^+$, $O^+$ and other heavier ions, these ions are less often hidden due to spacecraft charging, since for a given velocity their higher energy will make them less affected by the spacecraft potential. On average, $O^+$ dominates the global outflow of heavier ions. Estimates range from less than $10^{25}$ to more than $10^{26}$ ions s$^{-1}$, higher at higher geomagnetic activity and for more intense solar EUV radiation (Yau *et al* 1988, Yau and André 1997, Cully *et al* 2003, Peterson *et al* 2006, 2008, Parks *et al* 2015). An order of magnitude estimate of the average over a solar cycle is a few times $10^{25}$ ions s$^{-1}$. This would mean that for ions, $H^+$ dominates the number outflow, while $O^+$ dominates the mass outflow, at about 1 kg s$^{-1}$ (30 000 ton yr$^{-1}$).

Multiple mechanisms contribute to energization of outflowing ions (Wahlund *et al* 1992, André and Yau 1997, André *et al* 1998, Strangeway *et al* 2005, Moore and Horwitz 2007). As examples, energy can be transferred to the ionosphere from above, via Poynting flux (energy flux of electromagnetic waves) and via downgoing electrons accelerated in the magnetosphere. This can increase the electron temperature and hence the electron scale height, causing an ambipolar electric field starting an outflow of ions. For this process to continue dynamic effects are needed, such as horizontal convection of new ionospheric plasma into the region where such heating occurs. When the ions have reached collisionless altitudes other mechanisms can add energy, and the ions can obtain keV energies. Waves can heat the ions in the direction perpendicular to the magnetic field and the magnetic mirror force will then cause outflow in the diverging geomagnetic field. Ions can also be accelerated upward by the parallel electric fields causing downward energization of auroral electrons.

Above we have discussed only oxygen as the heavier particles (larger mass than hydrogen) originating from the atmosphere and ionosphere. In the thermosphere, above around 100 km, photodissociation of $O_2$ is fast, while recombination is slow. In contrast, the $N_2$ bond is more difficult to break directly, and should this happen the molecule is

rapidly regenerated through reactions with NO molecules (Strobel 2002). Although $N_2$ is more abundant than $O_2$ in the lower atmosphere, processes in the upper atmosphere make O and $O^+$ more common than the heavier $O_2$, $O_2^+$, $N_2$ and $N_2^+$ at a few 100 km (Ghosh 2002). The exobase is the altitude where collisions are no longer important, for Earth about 500 km. There are some observations of $N^+$ ions in the magnetosphere (Yau and André 1997) and some mass spectrometers on spacecraft do not have the resolution to distinguish between oxygen and nitrogen. While other species contribute, $O^+$ ions seem to dominate the outflow of heavier species. These ions are common around the exobase and non-thermal electromagnetic mechanisms can energize these ions.

## 8. Outflow of neutrals

To put the outflow of ions into perspective, we discuss the total mass outflow from planet Earth. Here we regard the solid Earth together with the collisional atmosphere and ionosphere as one system. Hence we disregard processes such as volcanism and combustion of fossil fuels and condensation into the hydro- and litospheres. The estimates for both outflow and inflow are still just order of magnitude calculations, see also Engwall (2009).

For the escape of neutrals, an obvious process is the loss of particles from the high-energy tail of the velocity distribution at the exobase. This thermal process is sometimes called Jeans escape (Jeans 1925). Estimating this process is complicated by the fact that particle distributions at the exobase are not Maxwellian at high energies due to the constant loss of particles. Using typical conditions at the exobase gives a global outflow of the order of $10^{26}$ particles $s^{-1}$ for H, much smaller for He, and yet again much smaller for heavier species such as O (Hunten and Strobel 1974, Hunten 2002, Strobel 2002).

The major non-thermal process leading to the escape of neutrals is charge exchange (Shizgal and Arkos 1996, Lie-Svendsen *et al* 1992). In typical reactions plasmaspheric protons (energy of the order of 1 eV) hit H or O atoms with much lower energies in the upper atmosphere. The resulting H atoms often have velocities above escape velocity, while the resulting oxygen atoms usually do not. (The escape velocity at the exobase is 11 km $s^{-1}$, which for H corresponds to an energy of 0.6 eV, and for the heavier O to nearly 10 eV). The estimated global order of magnitude outflow is similar to that of the neutral thermal outflow, $10^{26}$ particles $s^{-1}$, and again hydrogen dominates. The hydrogen originates mainly from the oceans, releasing oxygen into the atmosphere (Hanslmeier 2007, Engwall 2009).

## 9. Inflow

A large fraction of the mass inflow to planet Earth is from meteoroids and larger objects, hitting the atmosphere. Much of the number flux of material hitting the atmosphere comes in the form of small particles, less than about a mg, or one mm in radius (Love and Brownlee 1993, Ceplecha *et al* 1998). Different techniques are used to detect incoming particles of different sizes, and the inflow varies with location, day of the year and time during the day (Szasz *et al* 2004, Mann *et al* 2011). For observations in the atmosphere, meteor radars and optical camera networks are used (Ceplecha *et al* 1998, Flynn and Sutton 2006, Campbell-Brown *et al* 2012). Smaller particles can be measured by impact detectors on spacecraft (Love and Brownlee 1993). Also, studies of marine isotope records can be used to estimate the long term average inflow (Peucker-Ehrenbrink 1996).

Some contribution comes from much larger objects, such as the Chelyabinsk airburst 2013 and the Tunguska event 1908, caused by objects tens of meters across (Popova *et al* 2013).

To include larger and much less frequent impacts, lunar craters and observations of near-Earth asteroids can be taken into account (Ceplecha *et al* 1998). Over geological timescales large objects can dominate the average mass inflow and also carry enough energy to change the global conditions for life (Toon *et al* 1997). For a typical year, many estimates are consistent with a total inflow of at least a few tons $d^{-1}$ (100 g $s^{-1}$) to hundreds of tons $d^{-1}$ (a few kg $s^{-1}$) (Love and Brownlee 1993, Engwall 2009, Mann *et al* 2011, Plane 2012). This is similar to our estimates of the mass outflow from Earth.

Also charged particles can reach the collisional ionosphere. Electrons accelerated to keV energies cause auroras when they hit the upper atmosphere, but carry only a small mass flux. Some ions can also precipitate and cause so-called proton auroras (e.g. Frey *et al* 2003). Also, studies related to the investigations of outflowing low-energy ions show that many of these ions do not directly leave the magnetospheric system. Rather, they reach the plasma sheet (the current sheet in the magnetotail), are probably energized, and circulate in the magnetosphere (Haaland *et al* 2012a, Li *et al* 2012, 2013). However, statistics from low altitude spacecraft indicate that only a small fraction of these ions return to the ionosphere (Newell *et al* 2009). One reason that only a few ions reach the collisional ionosphere is that they have to travel downward nearly along the magnetic field, in the so-called loss-cone, in order not to be reflected by the magnetic mirror force.

## 10. Other planets, moons and exo-planets

The upper atmospheres of other solar system bodies are ionized in a way similar to what happens at Earth, creating ionospheres. In the case of Mars, with a well developed ionosphere but no global magnetic field, interaction with the solar wind leads to the formation of an induced magnetosphere. Observations during high solar activity with a Langmuir probe on Phobos-2 indicated regions of low-energy plasma and the total outflow was estimated to a few times $10^{25}$ ions $s^{-1}$ (Nairn *et al* 1991) consistent with recent analysis of particle detector data from the same spacecraft (Ramstad *et al* 2013). Some properties of low-energy ion outflows from the ionosphere can be detected with particle

instruments, e.g., on Mars Express (Lundin *et al* 2009) and careful statistical treatment including low energy particle data indicates an outflow of heavy ions during low solar activity of $2 \times 10^{24}$ ions $s^{-1}$ (Nilsson *et al* 2011) varying with solar EUV flux (Lundin *et al* 2013). However, results from the sounding radar MARSIS onboard Mars Express show high plasma densities in regions around Mars where almost no plasma is detected by particle instruments (Dubinin *et al* 2008). This suggests a situation similar to what is being revealed around Earth: low-energy plasmas are more important than previously anticipated. On Venus, the situation may be similar. Observations with Langmuir probes on Pioneer Venus Orbiter indicated regions of low-energy plasma (Brace *et al* 1987). Particle detectors give a global outflow of the order of $10^{25}$ ions $s^{-1}$ using Venus Express and Pioneer Venus Orbiter data (Barabash *et al* 2007, Fedorov *et al* 2011, Nordström *et al* 2013) but ions at a few eV cannot always be reliably detected with previous or present instruments. The planet sized moon Titan orbits most of the time inside the magnetosphere of Saturn. Langmuir probe data from multiple Titan flybys of the Cassini spacecraft indicate a plume of low-energy ionospheric plasma (Edberg *et al* 2011, Coates *et al* 2012). The associated outflow is estimated to around $10^{25}$ ions $s^{-1}$, showing the importance of low-energy plasma around yet another celestial body.

It is possible to detect the outflow of particles from planets from a distance, also for exo-planets orbiting distant stars. HD 209458b is a Jupiter-type gas giant planet orbiting its host star HD 209458, which is a solar-like G-type star with an age of about 4 Gyr. Absorption in the stellar Lyman-a line observed during the transit of HD 209458b in front of its host star reveals high-velocity atomic hydrogen at great distances from the planet (Vidal-Majar *et al* 2003) and the escape mechanisms are compared to mechanism in our solar system (Holmström *et al* 2008, Linsky *et al* 2010). Also studies of more Earth-like exoplanets in the habitable zone with temperatures suitable for liquid water are in progress (Kislyakova *et al* 2013). The evolution of atmospheres and ionospheres is an important factor when considering the conditions for biological life on other planets and moons (Yamauchi and Wahlund 2007, Lammer *et al* 2008, 2010). Parameters describing distant stars and planets vary, but the basic physical mechanisms remain the same. Understanding the outflow of planetary atmospheres in our solar system is one important piece in understanding the possibilities for life to evolve on exo-planets in the rest of the Galaxy.

## 11. Summary

The ion density and number flux in most of the volume of the Earth´s magnetosphere is dominated by low-energy (eV) positive ions from the ionsophere. Previously these ions could often not be detected on sunlit, positively charged, spacecraft. We use a technique based on the detection of the wake behind a charged spacecraft in a supersonic ion flow to detect these low-energy ions. Including this low-energy ion component gives a better map of the plasma abundance in near-Earth space. This updated map improves our understanding of plasma processes such as the speed of Alfvén waves and associated energy transport. This update also improves our knowledge concerning the rate and micro-physics of magnetic reconnection.

The order of magnitude global outflow of particles originating as low-energy ions, mainly $H^+$, is $10^{26}$ ions $s^{-1}$, increasing with geomagnetic activity and solar EUV radiation. This is similar to the estimates of thermal escape, and escape due to charge exchange, of mainly neutral hydrogen from the upper atmosphere. On average this gives an order of magnitude estimate of the global outflow of ionized and neutral hydrogen of a few times $10^{26}$ particles $s^{-1}$. The estimated number outflow of $O^+$ ions is more variable and lower, with an average around a few times $10^{25}$ particles $s^{-1}$. Due to their larger mass these particles might still dominate the average mass outflow, at around 1 kg $s^{-1}$. A large fraction of the mass outflow seems to be due to charged particles. One reason is that electromagnetic energy originating from the solar wind can give escape velocity to a small fraction of the upper ionosphere also when there is not at all enough energy to heat the bulk of the atmosphere.

The particle number inflow on a typical year is dominated by bodies smaller than about 1 mm in radius, with an estimated order of magnitude total mass inflow of about 1 kg $s^{-1}$. Hence, averaged over a solar cycle of about 11 yr, present reasonable order of magnitude estimates of the global mass outflow and inflow to Earth are similar, at 1 kg $s^{-1}$ (30 000 ton $yr^{-1}$).

The mass of Earth´s atmosphere is about $5 \times 10^{18}$ kg. Even without any inflow or supply from the litho- and hydrospheres, the present outflow on geological timescales of a Gyr corresponds to less than one percent of the total mass. On such long time scales, impacts of large (km) size asteroids and comets can be a major fraction of the mass inflow but can also remove significant parts of the atmosphere.

Several processes determine the stability of an atmosphere of a planet or large moon. Biological life as we know it benefits from a stable atmosphere. Understanding atmospheric and ionospheric outflow from Earth and other planets in our solar system is one important step to understand the possibilities for life to evolve on exo-planets around distant stars.

## Acknowledgments

This work was supported by SNSB contracts 170/12 and 93/14.

## References

Abe T, Yau A W, Watanabe S, Yamada M and Sagawa E 2004 Long-term variation of the polar wind velocity and its implication for the ion acceleration process: akebono/suprathermal ion mass spectrometer observations *J. Geophys. Res.* **109** A09305

André M and Yau A W 1997 Theories and observations of ion energization and outflow in the high latitude magnetosphere *Space Sci. Rev.* **80** 27–48
André M and Cully C M 2012 Low-energy ions: a previously hidden solar system particle population *Geophys. Res. Lett.* **39** L03101
André M, Li K and Eriksson A I 2015 Outflow of low-energy ions and the solar cycle *J. Geophys. Res. Space Phys.* **120** 1072–85
André M *et al* 1998 Ion energization mechanisms at 1700 km in the auroral region *J. Geophys. Res. Space Phys.* **103** 4199–222
André M *et al* 2010 Magnetic reconnection and cold plasma at the magnetopause *Geophys. Res. Lett.* **37** L22108
André N and Lemaire J F 2006 Convective instabilities in the plasma-sphere *J. Atmos. Sol.—Terr. Phys.* **68** 213–27
Aschwanden M J 2004 *Physics of the Solar Corona: An Introduction* (Berlin: Springer)
Axford W I 1968 The polar wind and the terrestrial helium budget *J. Geophys. Res.* **73** 6855–9
Balogh A *et al* 2001 The Cluster magnetic field investigation: overview of in-flight performance and initial results *Ann. Geophys.* **19** 1207–17
Banks P M and Holzer T E 1968 The polar wind *J. Geophys. Res.* **73** 6846–54
Barabash S *et al* 2007 The loss of ions from Venus through the plasma wake *Nature* **450** 650–3
Borovsky J E and Denton M H 2008 A statistical look at plasmaspheric drainage plumes *J. Geophys. Res.* **113** A09221
Brace L H *et al* 1987 The ionotail of Venus: its configuration and evidence for ion escape *J. Geophys. Res.* **92** 15–26
Brekke P and Broms F 2013 *Northern Lights: a Guide* (Forlaget Press)
Burchill J K *et al* 2010 Thermal ion upflow in the cusp ionosphere and its dependence on soft electron energy flux *J. Geophys. Res.* **115** A05206
Campbell-Brown M D, Kero J, Szasz C, Pellinen-Wannberg A and Weryk R J 2012 Photometric and ionization masses of meteors with simultaneous EISCAT UHF radar and intensified video observations *J. Geophys. Res.* **117** A09323
Ceplecha Z, Borovicka J, Elford W G, Revelle D O, Hawkes R L, Porubcan V and Simek M 1998 Meteor phenomena and bodies *Space Sci. Rev.* **84** 327–471
Chandler M O, Waite J H Jr and Moore T E 1991 Observations of polar ion outflows *J. Geophys. Res.* **96** 1421–8
Chandler M O *et al* 1999 Evidence of component merging equatorward of the cusp *J. Geophys. Res.* **104** 22623–33
Chappell C R 2015 The role of the ionosphere in providing plasma to the Terrestrial magnetosphere—an historical overview *Space Sci. Rev.* **195** 5–25
Chappell C R, Baugher C R and Horwitz J L 1980 New advances in thermal plasma research *Rev. Geophys. Space Phys.* **18** 853–61
Chappell C R, Moore T E and Waite J H Jr 1987 The ionosphere as a fully adequate source of plasma for the Earth's magnetosphere *J. Geophys. Res.* **92** 5896–910
Coates A J *et al* 2012 Cassini in Titan's tail: CAPS observations of plasma escape *J. Geophys. Res.* **117** A05324
Cully C M, Donovan E F, Yau A W and Arkos G G 2003 Akebono/suprathermal mass spectrometer observations of low-energy ion outflow: dependence on magnetic activity and solar wind conditions *J. Geophys. Res.* **108** 1093
Dandouras I 2013 Detection of a plasmaspheric wind in the Earth's magnetosphere by the Cluster spacecraft *Ann. Geophys.* **31** 1143
Darrouzet F *et al* 2008 Statistical analysis of plasmaspheric plumes with Cluster/WHISPER observations *Ann. Geophys.* **26** 2403–17
Darrouzet F *et al* 2009 Plasmaspheric density structures and dynamics: properties observed by the CLUSTER and IMAGE missions *Space Sci. Rev.* **145** 55–106
Dubinin E *et al* 2008 Structure and dynamics of the solar wind/ionosphere interface on mars: MEX-ASPERA-3 and MEX-MARSIS observations *Geophys. Res. Lett.* **35** L11103
Edberg N J T *et al* 2011 Structured ionospheric outflow during the Cassini T55-T59 Titan flybys *Planet. Space Sci.* **59** 788–97
Engwall E 2009 Low-energy ion escape from the Terrestrial polar regions *PhD Thesis* Uppsala university
Engwall E *et al* 2009a Earth's ionospheric outflow dominated by hidden cold plasma *Nat. Geosci.* **2** 24–7
Engwall E *et al* 2009b Survey of cold ionospheric outflows in the magnetotail *Ann. Geophys.* **27** 3185–201
Engwall E, Eriksson A I and Forest J 2006a Wake formation behind positively charged spacecraft in flowing tenuous plasmas *Phys. Plasmas* **13** 2904–13
Engwall E, Eriksson A I and Forest J 2006a *Phys. Plasmas* **13** 062904
Engwall E, Eriksson A I, André M, Dandouras I, Paschmann G, Quinn J and Torkar K 2006b Low-energy (order 10 eV) ion flow in the magnetotail lobes inferred from spacecraft wake observations *Geophys. Res. Lett.* **33** L06110
Eriksson A I *et al* 2006 Electric field measurements on cluster: comparing the double-probe and electron drift techniques *Ann. Geophys.* **24** 275–89
Escoubet C P, Fehringer M and Goldstein M 2001 Introduction: the cluster mission *Ann. Geophys.* **19** 1197–200
Fedorov A *et al* 2011 Measurements of the ion escape rates from Venus for solar minimum *J. Geophys. Res.* **116** A07220
Flynn G J and Sutton S R 2006 An assessment of the chemical heterogenity of individual ~3 $\mu$m fragments from an L2011 cluster IDP *Meteorit. Planet. Sci.* **37** (Suppl.) A48
Foerstner A 2007 *James Van Allen: The First Eight Billion Miles* (Iowa City: University of Iowa Press)
Frey H U, Mende S B, Fuselier S A, Immel T J and Ostgaard N 2003 Proton aurora in the cusp during southward IMF *J. Geophys. Res. Space Phys.* **108** 1277
Ghosh S N 2002 *The Neutral Upper Atmosphere* (Dordrecht: Kluwer)
Gillmore C S 1997 The formation and early evolution of studies of the magnetosphere *History of Geophys.* vol 7 (Washington DC: American Geophysical Union)
Gustafsson G *et al* 2001 First results of electric field and density observations by Cluster EFW based on initial months of operation *Ann. Geophys.* **19** 1219–40
Haaland S *et al* 2012a Estimating the capture and loss of cold plasma from ionospheric outflow *J. Geophys. Res.* **117** A07311
Haaland S, Svenes K, Lybekk B and Pedersen A 2012b A survey of the polar cap density based on Cluster EFW probe measurements: solar wind and solar irradiation dependence *J. Geophys. Res.* **117** A01216
Hanslmeier A 2007 *The Sun and Space Weather* 2nd edn (Berlin: Springer)
Hoffman J H 1970 Studies of the composition of the ionosphere with a magnetic deflection mass spectrometer *Int. J. Mass Spectrom. Ion Phys.* **4** 315–22
Holmström M *et al* 2008 Energetic neutral atoms as the explanation for the high-velocity hydrogen around HD209458b *Nature* **451** 970–2
Huddleston M M, Chappell C R, Delcourt D C, Moore T E, Giles B L and Chandler M O 2005 An examination of the process and magnitude of ionospheric plasma supply to the magnetosphere *J. Geophys. Res.* **110** A12202
Hunten D M 2002 Exospheres and planetary escape *Atmospheres in the Solar System: Comparatative Aeronomy* (*Geophysical Monograph* vol 130) (Washington, DC: American Geophysical Union) pp 191–2020
Hunten D M and Strobel D F 1974 Production and escape of terrestrial hydrogen *J. Atmos. Sci.* **31** 305–17
Jeans J H 1925 *The Dynamical Theory of Gases* 4th edn (New York: Cambridge University Press)

Kelley M C 2009 *The Earth's Ionosphere* (Amsterdam: Elsevier)
Kislyakova K G *et al* 2013 XUV exposed, non-hydrostatic hydrogen rich upper atmospheres of Terrestrial planets: II. Hydrogen coronae and ion escape *Astrobiology* **13** 1030–48
Kivelson G K and Russell C T 1995 *Introduction to Space Physics* (Cambridge: Cambridge University Press)
Koepke M E 2008 Interrelated laboratory and space plasma experiments *Rev. Geophys.* **46** RG3001
Koskinen H E J 2011 *Physics of Space Storms: From the Solar Surface to the Earth* (Berlin: Springer)
Kraus L and Watson K W 1958 Plasma motions induced by satellites in the ionosphere *Phys. Fluids* **1** 480
Lammer H *et al* 2008 Atmospheric escape and evolution of Terrestrial planets and satellites *Space Sci. Rev.* **139** 399–436
Lammer H *et al* 2010 Geophysical and atmospheric evolution of habitable planets *Astrobiology* **10** 45
Lee J H and Angelopoulos V 2014 On the presence and properties of cold ions near Earth's equatorial magnetosphere *J. Geophys. Res. Space Phys.* **119** 1749–70
Li K *et al* 2012 On the ionospheric source region of cold ion outflow *Geophys. Res. Lett.* **39** L18102
Li K *et al* 2013 Transport of cold ions from the polar ionosphere to the plasma sheet *J. Geophys. Res. Space Phys.* **118** 5467–77
Liao J, Kistler L M, Mouikis C G, Klecker B and Dandouras I 2012 Solar cycle dependence of the cusp $O^+$ access to the near-Earth magnetotail *J. Geophys. Res.* **117** A10220
Lie-Svendsen Ö, Rees M H and Stamnes K 1992 Helium escape from the Earth's atmosphere: the charge exchange mechanism revisited *Planet. Space Sci.* **40** 1639–62
Linsky *et al* 2010 Observations of mass loss from the transiting exoplanet HD209458b *Astrophys. J.* **717** 1291
Love S G and Brownlee D E 1993 A direct measurement of the Terrestrial mass accretion rate of cosmic dust *Science* **262** 550–3
Lundin R, Barabash S, Holmström M, Nilsson H, Futaana Y, Ramstad R, Yamauchi M, Dubinin E and Fraenz M 2013 Solar cycle effects on the ion escape from Mars *Geophys. Res. Lett.* **40** 6028–32
Lundin R *et al* 2009 Atmospheric origin of cold ion escape from Mars *Geophys. Res. Lett.* **36** L17202
Lybekk B, Pedersen A, Haaland S, Svenes K, Fazakerley A N, Masson A, Taylor M G G T and Trotignon J-G 2012 Solar cycle variations of the Cluster spacecraft potential and its use for electron density estimations *J. Geophys. Res.* **117** A01217
Mann I *et al* 2011 Dusty plasma effects in near Earth space and interplanetary medium *Space Sci. Rev.* **161** 1–47
Matsui H *et al* 1999 Cold dense plasma in the outer magnetosphere *J. Geophys. Res.* **104** 25077–95
Milan S E, Gosling J S and Hubert B 2012 Relationship between interplanetary parameters and the magnetopause reconnection rate quantified from observations of the expanding polar cap *J. Geophys. Res.* **117** A03226
Milan S E, Hutchinson J, Boakes P D and Hubert B 2009 Influences on the radius of the auroral oval *Ann. Geophys.* **27** 2913–24
Miyake Y, Cully C M, Usui H and Nakashima H 2013 Plasma particle simulations of wake formation behind a spacecraft with thin wire booms *J. Geophys. Res. Space Phys.* **118** 5681–94
Moore T E and Horwitz J L 2007 Stellar ablation of planetary atmospheres *Rev. Geophys.* **45** RG3002
Moore T E *et al* 2008 Plasma plume circulation and impact in an MHD substorm *J. Geophys. Res.* **113** A06219
Nairn C M, Grard R, Skalsky A and Trotignon J G 1991 Plasma and wave observations in the night sector of Mars *J. Geophys. Res.* **96** 11227–33
Newell P T, Sotirelis T and Wing S 2009 Diffuse, monoenergetic, and broadband aurora: the global precipitation budget *J. Geophys. Res.* **114** A09207
Nilsson H, Barghouthi I A, Slapak R, Eriksson A I and André M 2012 Hot and cold ion outflow: spatial distribution of ion heating *J. Geophys. Res.* **117** A11201
Nilsson H, Barghouthi I A, Slapak R, Eriksson A I and André M 2013 Hot and cold ion outflow: observations and implications for numerical models *J. Geophys. Res. Space Phys.* **118** 105–17
Nilsson H *et al* 2011 Heavy ion escape from Mars, influence from solar wind conditions and crustal magnetic fields *Icarus* **215** 475–84
Nordström T, Stenberg G, Nilsson H, Barabash S and Zhang T L 2013 Venus ion outflow estimates at solar minimum: influence of reference frames and disturbed solar wind conditions *J. Geophys. Res. Space Phys.* **118** 3592–601
Ogawa Y, Häggström I, Buchert S C, Oksavik K, Nozawa S, Hirahara M, van Eyken A P, Aso T and Fujii R 2009 On the source of the polar wind in the polar topside ionosphere: first results from the EISCAT Svalbard radar *Geophys. Res. Lett.* **36** L24103
Olsen R C 1982 The hidden ion population of the magnetosphere *J. Geophys. Res.* **87** 3481–8
Olsen R C, Chappell C R, Gallagher D L, Green J L and Gurnett D A 1985 The hidden ion population: revisited *J. Geophys. Res.* **90** 12121–32
Parks G K, Lee E, Fu S Y, Fillingim M, Dandouras I, Cui Y B, Hong J and Rème H 2015 Outflow of low-energy $O^+$ ion beams observed during periods without substorms *Ann. Geophys.* **33** 333–44
Paschmann G, Oieroset M and Phan T 2013 *In-situ* observations of reconnection in space *Space Sci. Rev.* **178** 385–417
Paschmann G *et al* 2001 The electron drift instrument on Cluster: overview of first results *Ann. Geophys.* **19** 1273–88
Pedersen A *et al* 2008 Electron density estimations derived from spacecraft potential measurements on cluster in tenuous plasma regions *J. Geophys. Res.* **113** A07S33
Peterson W K, Collin H L, Lennartsson O W and Yau A W 2006 Quiet time solar illumination effects on the fluxes and characteristic energies of ionospheric outflow *J. Geophys. Res.* **111** A11S05
Peterson W K, Andersson L, Callahan B C, Collin H L, Scudder J D and Yau A W 2008 Solar-minimum quiet time ion energization and outflow in dynamic boundary related coordinates *J. Geophys. Res.* **113** A07222
Peucker-Ehrenbrink B 1996 Accretion of extraterrestrial matter during the last 80 million years and its effect on the marine osmium isotope record *Geochim. Cosmochim. Acta* **60** 3187–96
Plane J M C 2012 Cosmic dust in the Earth´s atmosphere *Chem. Soc. Rev.* **41** 6507–18
Popova O P *et al* 2013 Chelyabinsk airburst, damage assessment, meteorite recovery, and characterization *Science* **342** 1069–73
Priest E and Forbes T 2000 *Magnetic Reconnection* (Cambridge: Cambridge University Press)
Ramstad R, Futaana Y, Barabash S, Nilsson H, del Campo B S M, Lundin R and Schwingenschuh K 2013 Phobos 2/ASPERA data revisited: planetary ion escape rate from Mars near the 1989 solar maximum *Geophys. Res. Lett.* **40** 477–81
Rand S 1960 Damping of the satellite wake in the ionosphere *Phys. Fluids* **3** 588
Sharp R D, Johnson R G and Shelley E G 1977 Observation of an ionospheric acceleration mechanism producing energetic (keV) ions primarily normal to the geomagnetic field *J. Geophys. Res.* **82** 3324–8
Shelley E G, Johnson R G and Sharp R D 1972 Satellite observations of energetic heavy ions during a geomagnetic storm *J. Geophys. Res.* **77** 6104–10
Shizgal B D and Arkos G G 1996 Non-thermal escape of the atmospheres of Venus, Earth and Mars *Rev. Geophys.* **34** 483–505

Spasojevic M and Sandel B R 2010 Global estimates of plasmaspheric losses during moderate disturbance intervals *Ann. Geophys.* **28** 27–36

Strangeway R J, Ergun R E, Su Y-J, Carlson C W and Elphic R C 2005 Factors controlling ionospheric outflows as observed at intermediate altitudes *J. Geophys. Res.* **110** A03221

Strobel D F 2002 Aeronomic systems on planets, moons, and comets *Atmospheres in the Solar System, Comparatative Aeronomy* (*Geophysical Monograph* vol 130) (Washington, DC: American Geophysical Union) pp 7–22

Su Y-J *et al* 1998 Polar wind survey with the thermal ion dynamics experiment/plasma source instrument suite aboard POLAR *J. Geophys. Res.* **103** 29305–37

Svenes K R, Lybekk B, Pedersen A and Haaland S 2008 Cluster observations of near-Earth magnetospheric lobe plasma densities—a statistical study *Ann. Geophys.* **26** 2845–52

Szasz C, Kero J, Pellinen-Wannberg A, Mathews J D, Mitchell N J and Singer W 2004 Latitudinal variations of diurnal meteor rates *Earth Moon Planets* **95** 101–7

Toledo-Redondo S, Vaivads A, André M and Khotyaintsev Y V 2015 Modification of the Hall physics in magnetic reconnection due to cold ions at the Earth's magnetopause *Geophys. Res. Lett.* **42** 6146–54

Toon O B, Zahnle K, Morrison D, Turco R P and Covey C 1997 Environmental perturbations caused by the impacts of asteroids and comets *Rev. Geophys.* **35** 41–78

Torkar K *et al* 2001 Active spacecraft potential control for Cluster-implementation and first results *Ann. Geophys.* **19** 1289–302

Van Allen J A and Frank L A 1959 Radiation around the Earth to a radial distance of 107 400 km *Nature* **183** 430–4

Vidal-Majar A *et al* 2003 An extended upper atmosphere around the extrasolar planet HD209458b *Nature* **422** 143–6

Wahlund J-E *et al* 1992 EISCAT observations of topside ion outflows during auroral activity: Revisited *J. Geophys. Res. Space Phys.* **97** 3019–37

Yamauchi M and Wahlund J-E 2007 Role of the ionosphere for the atmospheric evolution of planets *Astrobiology* **7** 783

Yau A W and André M 1997 Sources of ion outflow in the high latitude ionosphere *Space Sci. Rev.* **80** 1–25

Yau A W, Abe T and Peterson W K 2007 The polar wind: recent observations *J. Atmos. Sol.—Terr. Phys.* **69** 1936–83

Yau A W, Peterson W K and Shelley E G 1988 Quantitative parametrization of energetic ionospheric ion outflow *Geophys. Monogr. Ser.* **44** 211